PAPER

Check for updates

Tungstic acid-functionalized polycalix[4]resorcinarene as a cavity-containing hyper-branched supramolecular and recoverable acidic catalyst in 4*H*-pyran synthesis†

Aref Mahmoudi Asl, [ID] Bahador Karami [ID] * and Zahra Karimi [ID]

In this study, tungstic acid immobilized on polycalix[4]resorcinarene, PC4RA@SiPr−OWO₃H, as a mesoporous acidic solid catalyst was synthesized and investigated for its catalytic activity. Polycalix[4]resorcinarene was prepared *via* a reaction between formaldehyde and calix[4]resorcinarene, and then the resulting polycalix[4]resorcinarene was modified using (3-chloropropyl)trimethoxysilane (CPTMS) to obtain polycalix[4]resorcinarene@(CH₂)₃Cl that was finally functionalized with tungstic acid. The designed acidic catalyst was characterized by various methods including FT-IR spectroscopy, energy-dispersive X-ray spectroscopy (EDS), scanning electron microscopy (FE-SEM), X-ray diffraction (XRD), thermogravimetric analysis (TGA), elemental mapping analysis and transmission electron microscopy (TEM). The catalyst efficiency was evaluated *via* the preparation of 4*H*-pyran derivatives using dimethyl/diethyl acetylenedicarboxylate, malononitrile, and beta-carbonyl compounds, confirmed by FT-IR spectroscopy and ¹H and ¹³C NMR spectroscopy. The synthetic catalyst was introduced as a suitable catalyst with high recycling power in 4*H*-pyran synthesis.

Introduction

Over recent decades, calixarenes, especially calix[4]resorcinarene, an attractive set of macrocyclic molecules, have widely been used in molecular chemistry.[1,2] The production of this group of compounds results from the reaction between formaldehyde and phenol or its derivatives.[3] High thermal and chemical resistance, high melting point, non-toxicity, low solubility, and optical activity are among the remarkable properties of calixarenes.[4,5] Specific properties, such as green synthetic methods, possibility of derivatization, easy modification,[6] and ability to adjust their size, have introduced calixarenes in different dimensions as multifaceted structures, producing complex and fundamental scaffolds for various applications.[7]

The presence of two edges in their body has given these macromolecules outstanding features. The phenolic rings and substitution of hydroxy groups on phenyl rings involve the upper and lower edges, respectively. A hydrophobic cavity[8] is formed between the two edges through aromatic rings. This unique structure makes the calixes act as a basket.[9,10] Selective interactions and the formation of host-guest complexes are allowed to accept guest molecules, such as neutral molecules

and ions. Through pores in the structure of calixarenes,[11] they can recognize molecular guests and show attractive and appropriate functions.[12–17]

Calixarenes can be employed for different applications including the production of suitable catalysts according to the need for organic reactions, biological systems, binding to the substrate, HPLC stationary phases, heavy nanocapsules, metal adsorption agents, drug delivery materials, extraction of metal ions, detectors, ion transporters, and chemical sensors by changing the available spaces on them.[18–23]

High-performance catalysts are an essential component that the world strongly needs.[24] However, although homogeneous catalysts have attracted much attention, their use in chemical reactions has been restricted due to their high cost, low environmental safety and security, corrosion, and recovery. Recently, mixtures of organic acid catalysts and various solid supports, such as carbon, silica, and polymers, have been considered as desirable hybrids.[25]

The ability to transfer mass between raw materials and products, control the amount of solubility in aqueous solutions, produce a changeable hydrophobic space, separation, and other characteristics of polymer-supported catalysts do not exist in ordinary types.[26] Meanwhile, many polymeric supports suffer from several defects in different stages of synthesis, such as high synthesis time, a large number of production steps, and several defects in functionalization stages, such as lack of excellent thermal and chemical resistance, functionalization *via*

Department of Chemistry, Yasouj University, P. O. Box 353, Yasouj, 75918-74831, Iran. E-mail: karami@yu.ac.ir; Tel: +98-7431004000

co-polymerization or further post-polymerization under harsh reaction conditions, and solubility in different solvents.[27]

It is worth noting that the use of calixarenes to prepare heterogeneous catalysts for chemical changes is less known.[28,29] The non-covalent interactions of calixarenes including hydrophobic interactions, hydrogen bonding, and ionic–polar interactions provide a strong backbone for constructing polymer matrices.[30]

Porous organic polymers with tunable pores and large and stable specific surface areas significantly affect many fields including catalysts, drug carriers, and gas absorbers.[31–34] However, polymers based on calixarenes have rarely been studied in chemical reactions as catalysts so far.[35] Developing an efficient, practical, and environmentally safe method for designing biological and synthetic molecules is the principal goal of modern organic synthesis.

Due to the high significance of compounds bearing pyran structures, in the last decade, researchers have built increasingly modern methods for the synthesis of these compounds.[36] Pyrans are a substantial category of heterocycles as their core segments are included in a great diversity of biologically active compounds and natural products. Pyrans have a wide range of medicinal properties such as antioxidant, anti-microbial, anti-cancer, anti-HIV, anti-tumour, and anti-fungal activities.[37,38] Moreover, compounds with a pyran in their structure are widely applied in cosmetics as pigments and eco-friendly agricultural chemicals. The above-mentioned factors have caused to present various methods for their preparation.[39] Synthesizing this pyran class has been done by infrequent catalysts including homogeneous catalysts L-proline,[40] CH_3NH_2,[41] Na_2CO_3,[42] and borax.[43] Difficult recycling from the reaction media, prolonged reaction time, and biodegradation are among their disadvantages. Although heterogeneous catalysts such as $Fe_3O_4@SiO_2–NH_2$ (ref. 44) and $CuFe_2O_4$ (ref. 45) NPs do not have recycling issues, problems such as sensitivity to an acidic environment and high temperatures to carry out the reaction are their main disadvantages.[46,47] Considering the above-mentioned results and the continuing research of our group on heterogeneous catalysts, in this report, we present tungstic acid immobilized on the polycalix[4]resorcinarene surface, PC4RA@SiPr–OWO$_3$H, followed by the evaluation of its efficiency with regard to power, recyclability, and stability. Then it was employed in the reaction of malononitrile, dimethyl/diethyl acetylene dicarboxylate (DMAD/DEAD), and beta-carbonyls in water as an eco-friendly solvent at 45 °C.
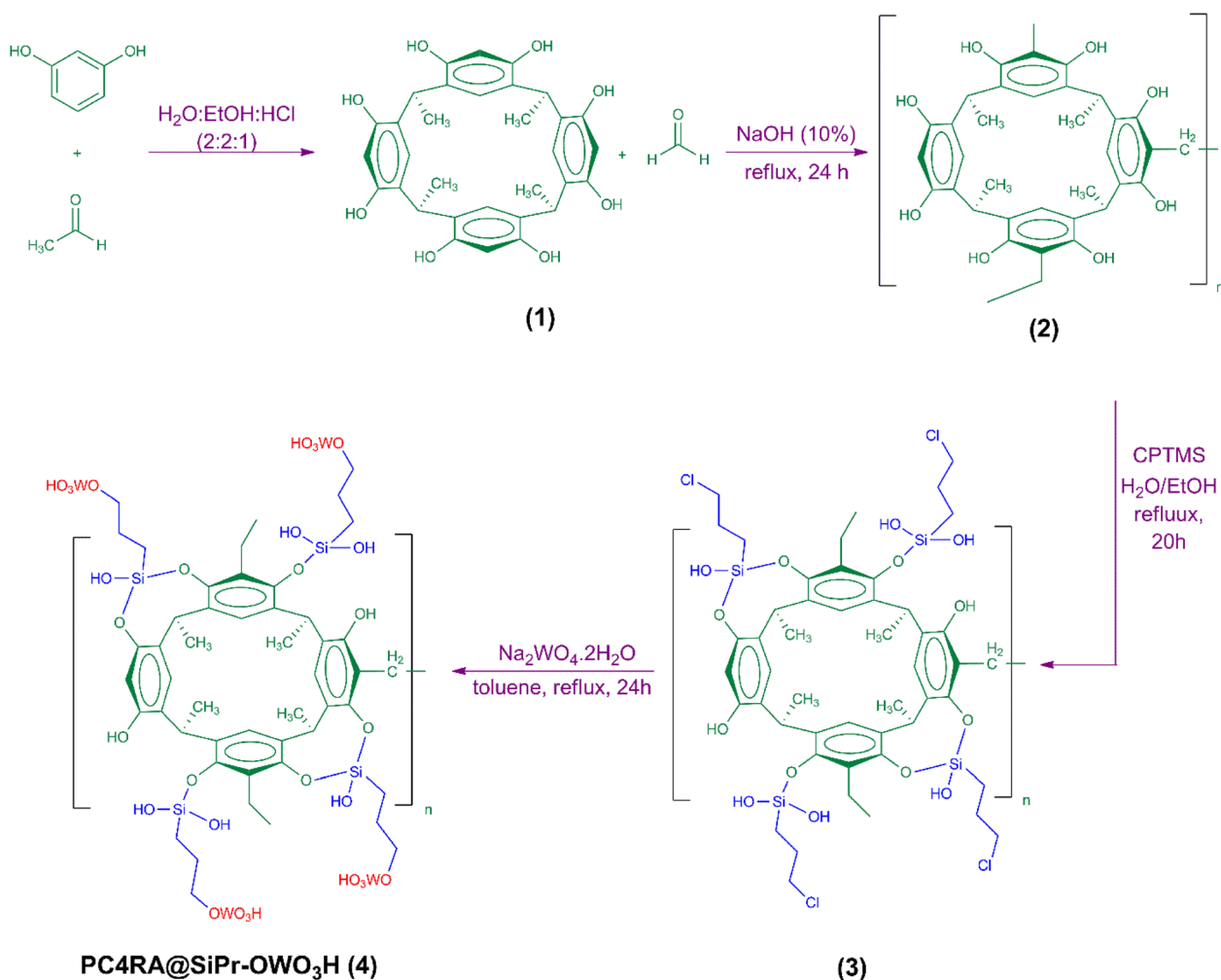
Scheme 1 Schematic steps of the synthesis of PC4RA@SiPr−OWO$_3$H catalysts.

Experimental

Materials

All used materials were prepared and purchased from Merck, Fluka and Aldrich chemical companies. The obtained results and data were verified by comparison with previous reports. A TLC plate (SIL G/UV254) was employed to recognize the reaction completion. An electrothermal apparatus (KSB1N) device was applied to confirm the melting point. A Fourier transform infrared spectrometer (JASCO FT-IR/680 plus) with KBr pellets was used to record the FT-IR spectrum of the compounds. A field-emission scanning electron microscope (FE-SEM Quanta 200 FEG, manufactured by FEI American) and a transmission electron microscope (TEM) equipped with an EM 200 apparatus from Philips were applied to determine the particle morphology and replacement of particles. X-ray powder diffraction (XRD) was performed using a Rigaku Ultima IV device manufactured by Japan. ^{1}H NMR and ^{13}C NMR spectra were recorded in a DMSO-d_6 solvent in the presence of tetramethylsilane as an internal standard using a Bruker Avance device at 300 and 75 MHz, respectively. A thermal analysis device (TGA) model (PerkinElmer STA6000) made by an American company was used to assess the thermal stability.

Synthesizing C4RA (1)

C4RA (1), calix[4]resorcinarene production, was prepared and applied based on previous reports.[48]

Synthesizing polycalix (2)

After preparing the mentioned bowl-like calix[4]resorcinarene, to synthesize the polymer (2) in question, 18 mmol of formaldehyde was added to 6 mmol of calix[4]resorcinarene (1) in a round-bottom flask containing 25 ml aqueous solution of NaOH (10%). The resulting mixture was stirred at a temperature of 90 °C for about 24 hours under an argon atmosphere and then treated with a 0.1 M HCl solution and converted into an acidic form. The obtained solid was collected and dried.[49]

Synthesizing PC4RA@SiPrCl (3)

First, 0.5 g of the synthesized polycalix (2) was dispersed in H$_2$O/EtOH (1 : 1) and then 1.7 g of CPTMS (8 mmol) was added into the prepared mixture, followed by refluxing under an argon atmosphere for 20 hours. After filtration, the remaining solid was washed with solvents (toluene, water and ethanol, respectively). The resulting solid was finally dried using an oven at a temperature of 80 °C for 10 hours.

Synthesizing PC4RA@SiPr–OWO$_3$H (4)

First, 0.6 g of the prepared PC4RA@SiPrCl (3) was placed into a round-bottom flask containing 10 ml of toluene. Then, 0.3 g of Na$_2$WO$_4$·2H$_2$O was added to the above-mentioned combination and stirred for 24 hours under argon and reflux conditions. The synthesized catalyst was washed with diethyl ether and water/ethanol (1 : 1) respectively and then dried at 100 °C. The obtained solid was first stirred in (25 ml, 0.1 N) HCl at room temperature for 1 hour. In the next step, it was washed first with toluene and then with water. The catalyst was extracted and dried at 80 °C for 5 hours (Scheme 1).

General method for the synthesis of *4H*-pyran derivatives

A mixture of malononitrile, DMAD/DEAD, and beta-carbonyls was reacted in the presence of 0.03 g acidic catalyst in water. The raw mixture was stirred at 45 °C for a needed time. The progress of the reaction was checked by TLC. After the reaction
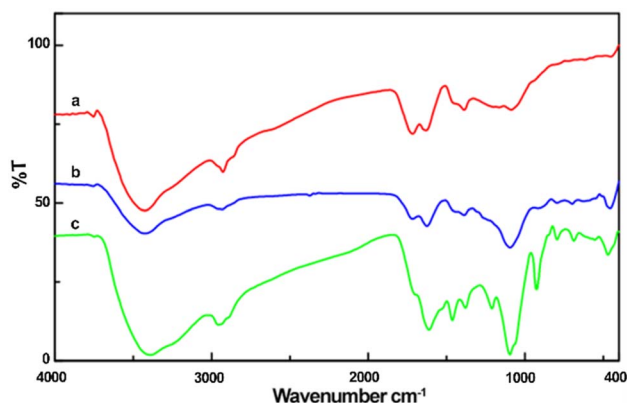

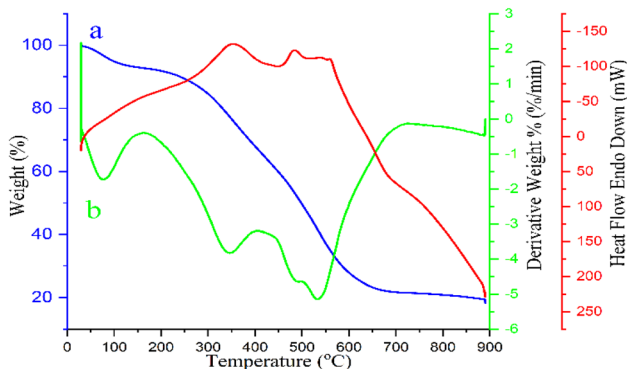**Fig. 1** FT-IR spectra of (a) polycalix, (b) PC4RA@SiPrCl and (c) PC4RA@SiPr–OWO$_3$H.

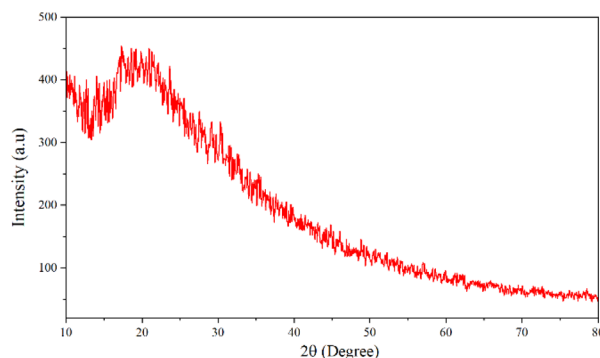**Fig. 2** TG analysis of PC4RA@SiPr–OWO$_3$H.

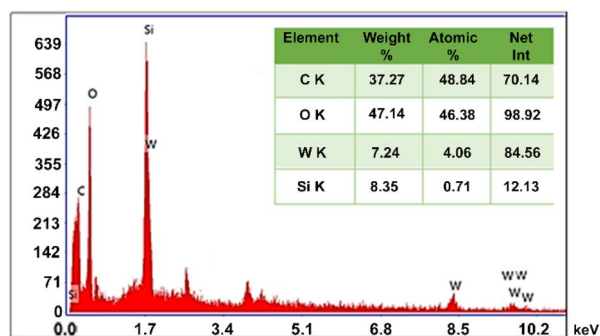**Fig. 3** XRD analysis of PC4RA@SiPr–OWO$_3$H.
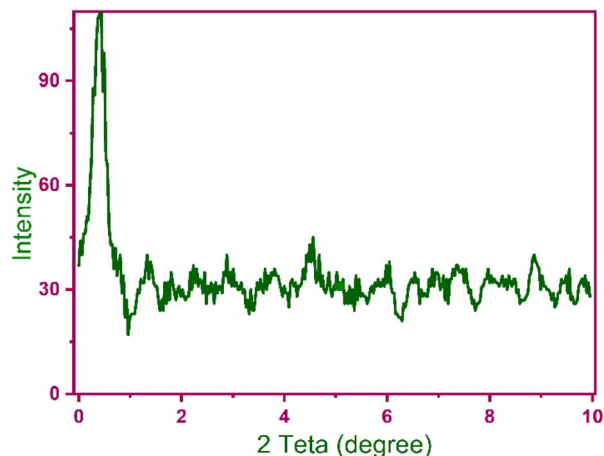
Fig. 4 LPXRD analysis of PC4RA@SiPr−OWO$_3$H.

Fig. 5 EDX pattern of PC4RA@SiPr−OWO$_3$H.

completion, the sediment formed in the container was washed with water and then recrystallized in ethanol. The results were analyzed and confirmed.

Results and characterization

In the context of increasing attention on heterogeneous catalysis for introducing green and beneficial procedures in chemical conversions, our group encouraged to prepare an eco-friendly and practical method for generating several 4*H*-pyran derivatives using a new tungstic acid–functionalized nano-scale polymeric catalyst based on C4RA as a highly active heterogeneous material. The designed acidic catalyst was synthesized and characterized by FT-IR spectroscopy, elemental mapping, EDX, FE-SEM, TGA, XRD, and TEM analyses.
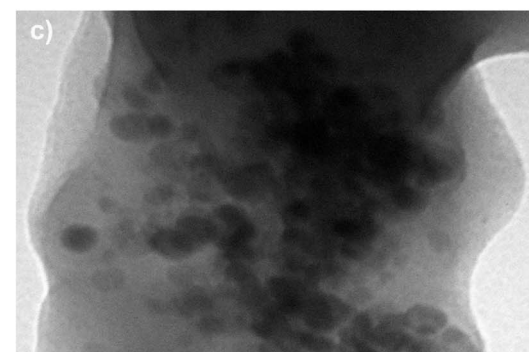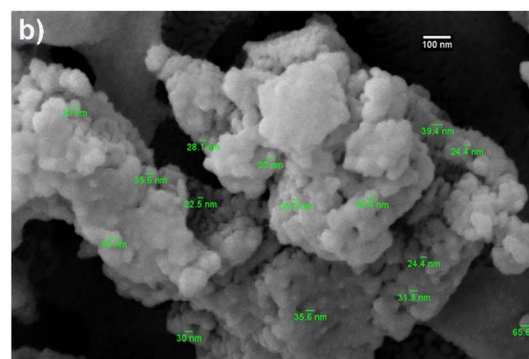

Fig. 6 Elemental mapping analysis of PC4RA@SiPr−OWO$_3$H.

Fig. 7 (a and b) SEM, (c) TEM images of PC4RA@SiPr−OWO$_3$H.

Table 1　Assessment of different parameters in preparing 4*H*-pyran derivatives[a]

Entry	Catalyst (g)	Solvent	T (°C)	Time (min)	Yield[b] (%)
1	0.03	MeOH	45	50	42
2	0.03	EtOH	45	30	58
3	0.03	EtOH/H$_2$O	45	25	71
4	0.03	Toluene	45	65	—
5	0.03	CH$_2$Cl$_2$	45	65	—
6	0.03	—	45	120	—
7	0.03	H$_2$O	45	15	96
8	0.02	H$_2$O	45	15	64
9	0.04	H$_2$O	45	15	85
10	0.03	H$_2$O	r.t	15	20
11	0.03	H$_2$O	65	15	94
12	0.03	H$_2$O	85	15	94
13	—	H$_2$O	45	160	—
14	PC4RA (0.03 g)	H$_2$O	45	65	20
15	PC4RA@SiPrCl (0.03 g)	H$_2$O	45	65	—
16	H$_2$WO$_4$ (0.03 g)	H$_2$O	45	65	53

[a] Condition: 1 : 1 ratio of malononitrile, beta-carbonyl and coumarin. [b] Isolated yields.
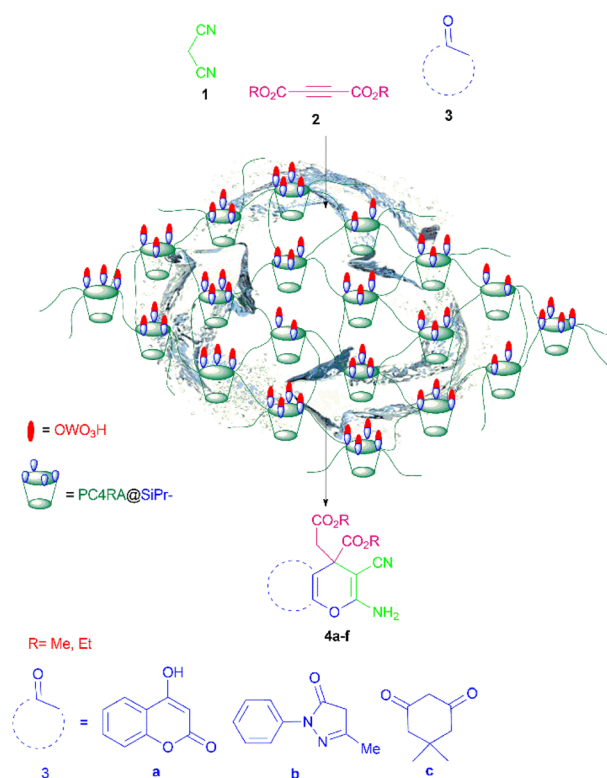
Scheme 2　Synthesis of 4*H*-pyran derivatives *via* a one-pot reaction using the polymeric catalyst PC4RA@SiPr−OWO$_3$H.

The FT-IR spectra of PC4RA, PC4RA@SiPrCl, and PC4RA@-SiPr−OWO$_3$H are depicted in Fig. 1. The study of each stage spectrum shows the accurate graft of the main components on the polymer structure. The peaks, related to symmetric and asymmetric stretching of the Si–O–Si bond, appeared at 1103 cm^{-1} and 794 cm^{-1}, respectively, confirming the successful connection of CPTMS as a modification linker to the polymer network. In the final stage of stabilization of tungstic acid to develop PC4RA@SiPr–OWO$_3$H, a new peak appeared at 890 cm^{-1} assigned to the W=O groups. The broad signals appearing at 3200–3450 cm^{-1} were attributed to the uncoated and acidic OH groups.
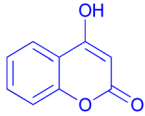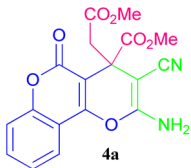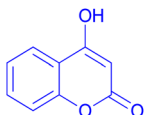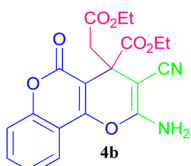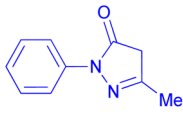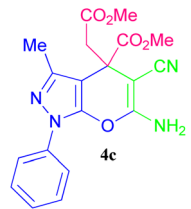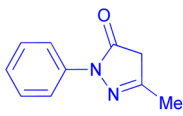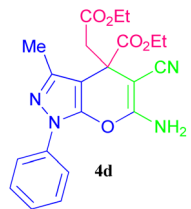
The TG analysis was used for the determination of the thermal stability of the catalyst under a nitrogen atmosphere. A relatively small weight loss at around 90 °C, in the TG curve spectrum, is apparent (Fig. 2a), attributed to the disposal of water molecules trapped in the pores of the catalyst structure, which is a natural phenomenon. There are three weight losses between 340 and 650 °C, showing two sharp cleavages at 340 and 490 °C, related to the breakdown of the inorganic moieties and the coupling agent. This graph shows that the thermal stability of the polymer system is up to 650 °C. The DTG curve provides additional information about the thermal stability of the functionalized polymer (Fig. 2b). The >650 °C temperature is related to the decomposition of the polymer unit. TG analysis verified good immobilization of groups on the polymer network.
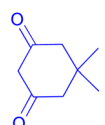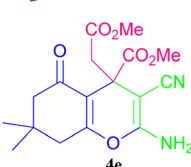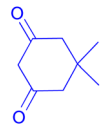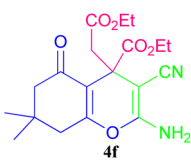
The XRD pattern of PC4RA@SiPr–OWO$_3$H, exhibited in Fig. 3, delivers a broad peak around $2\theta \approx 16$–$23°$, demonstrating amorphous polymeric support. The presence of crystalline phase of tungstic acid on the surface of the polymer is about $2\theta \approx 22°$ overlapped with the mentioned broad peak.

Fig. 4 exhibits the low-angle powder X-ray diffraction (LPXRD) analysis of the PC4RA@SiPr–OWO$_3$H structure. As witnessed in this curve, the strong peak that arose at $2\theta \approx 0.5°$

Table 2 4H-Pyrans preparing using PC4RA@SiPr–OWO$_3$H under optimized conditions

| Entry	R	Substrate	Product	Time (min)	Yield[a] (%)	M_p (°C)
1	Me		**4a**	15	96	206–208 (ref. 45)
2	Et		**4b**	21	87	206–208 (ref. 45)
3	Me		**4c**	25	93	198–200 (ref. 45)
4	Et		**4d**	28	85	112–114 (ref. 45)
5	Me		**4e**	19	91	180–182 (ref. 45)
6	Et		**4f**	21	86	230–232 (ref. 45)

[a] Isolated yields.

ascertains that the desired polymeric support, carrying SiPr–OWO$_3$H, owns a mesoporous structure.

Energy-dispersive X-ray spectroscopy (EDX) is one of the analyses used to characterize the structure of PC4RA@SiPr–OWO$_3$H. The pattern revealed that the regarded elements including C, O, W, and Si existed in the designed polymeric material, proving the successful connection of the raw materials on the surface of the desired catalyst (Fig. 5).

Moreover, elemental mapping was applied to exhibit the uniform distribution of the constituent elements. As shown in Fig. 6, all components (C, Si, O, and W) have homogeneously distributed throughout the structure, confirming FT-IR and TGA results.

SEM and TEM are techniques that can be relied upon to investigate the morphology of polymeric catalysts and the placement of nanoparticles on the surface as well. The images obtained from SEM reveal an amorphous structure containing uniform particles with an average size of nearly 55 nm and pores in the mesopore range (Fig. 7a and b). TEM analysis also indicates the amorphous support bearing the well-made connection of acidic moieties on it, confirming the results of SEM images (Fig. 7c). The polymeric catalyst was tested by synthesizing some 4H-pyran derivatives to check its effect and performance. For this purpose, the reaction of malononitrile, DMAD, and 4-hydroxycoumarin was used as the model reaction, producing 4a. First, solvent optimization was performed to
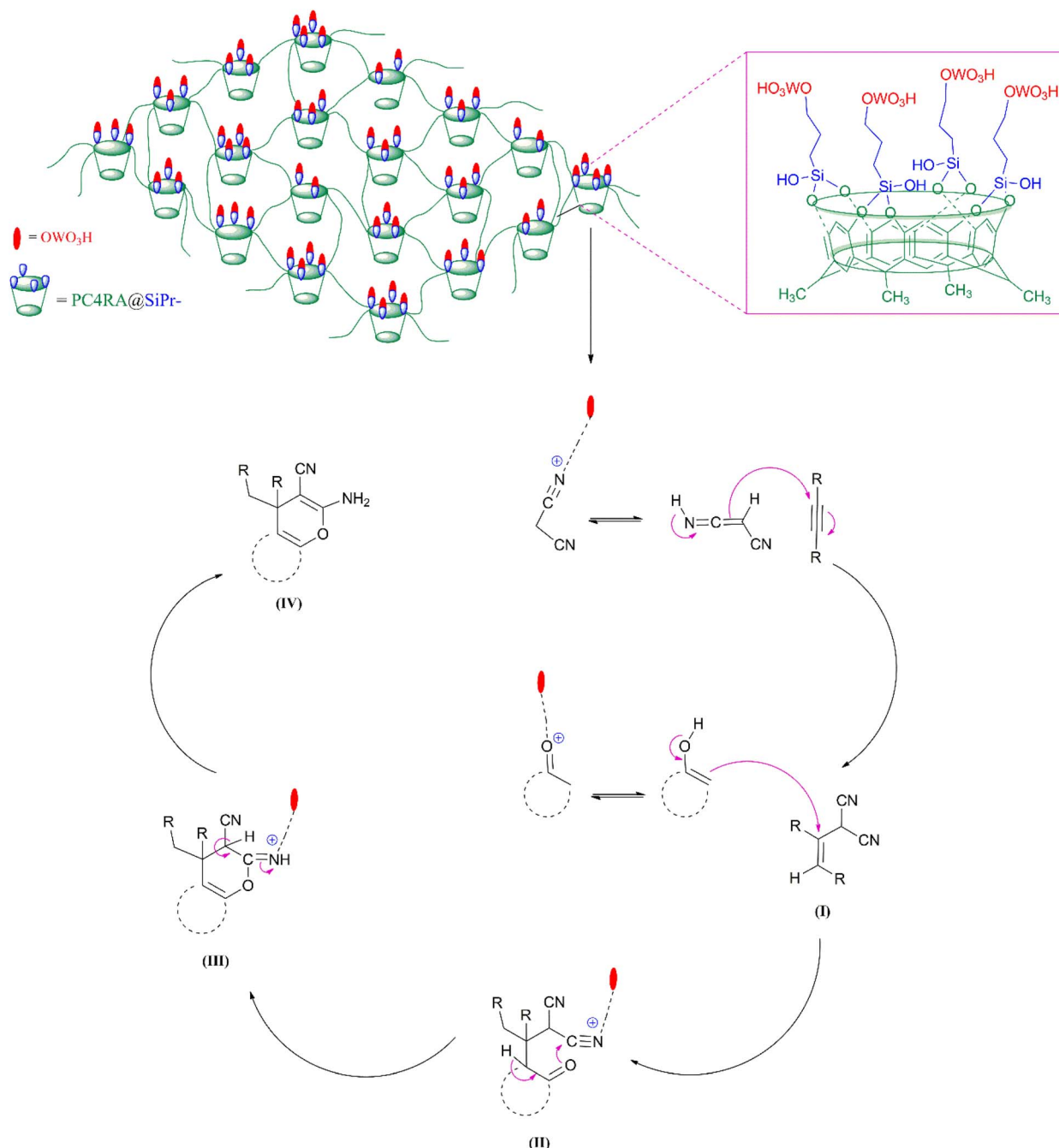
Scheme 3 Proposed mechanism of action of the PC4RA@SiPr−OWO$_3$H catalyst in the synthesis of 4*H*-pyran derivatives.

increase the catalyst utilization capacity. After investigating various solvents such as H$_2$O, MeOH, EtOH, toluene, CH$_2$Cl$_2$ and solvent-free conditions, the best performance was acquired in water, producing the selected product 4a with high yields compared to other solvents (Table 1, entries 1–6). Optimizing the catalyst loading showed that the most appropriate amount of catalyst (required per mmol with a 1 : 1 ratio of raw materials to progress the reaction) is 0.03 g, which indicates high catalyst performance (Table 1, entries 7–9). In the next step, the assessment continued to find the optimal temperature. Due to the good speed of the catalyst at low temperatures, there is no

need for high temperature to complete the reaction (Table 1, entries 10–12). Finally, to indicate OWO$_3$H as the active site of the polymeric catalyst, the model reaction was carried out in the presence of PC4RA and PC4RA@SiPrCl, resulting in trace yields compared with PC4RA@SiPr−OWO$_3$H, proving that OWO$_3$H moieties act as active portions (Table 1, entries 14–15). The homogeneous phase was examined by H$_2$WO$_4$ to catalyze the model reaction, obtaining only 53% yield of the corresponding product, confirming that OWO$_3$H acts as an active site but in corporation with a cavity-containing polymeric support (PC4RA), enhancing the reactivity (Table 1, entries 16 *versus*

entries 7). Since the evaluation and analysis of the designed catalyst exhibited promising results, in the next step, for using the apparent advantages, PC4RA@SiPr–OWO$_3$H was applied to catalyze more of this kind of compound (Scheme 2).

As shown in Table 2, PC4RA@SiPr–OWO$_3$H successfully yielded 4H-pyran derivatives using a cavity-containing unique structural form coupled with tungstic acid in its body; furthermore, it completed this reaction without forming side products and in a considerably shorter time than that reported previously. The ^{1}H NMR, ^{13}C NMR, and FT-IR spectra of the 4H-pyran are reported in the ESI file.†

As shown in the proposed mechanism in Scheme 3, the synthesis of 4H-pyrans was carried out through 4 sequence steps with three intermediates in the presence of PC4RA@SiPr–OWO$_3$H. The initial condensation of malononitrile with DMAD results in intermediates (I) by the Michael addition. Next, the nucleophilic addition of activated beta-carbonyl to (I) leads to the formation of Michael adduct (II). Finally, compound (III) was obtained from intramolecular cyclization, generating compound (IV).

The recyclability of the catalyst was investigated using the presented reaction in Table 1 as a model reaction. The insolubility in organic and aqueous solvents and the high stability of the catalyst make it possible to be separated easily from the reaction mixture. At the end of the reaction, the catalyst was separated from the reaction mixture using filter paper, washed, dried and then eventually used in the Re-reactions under the optimized situations. The mentioned operation was repeated and examined eight times in turns. The results indicated that the catalyst afforded to progress the reaction without reducing its initial activity, indicating high stability and excellent immobilization of functionalities on the surface of the polymeric catalyst (Fig. 8). FT-IR, EDX, elemental mapping, and TEM analyses were performed to reveal the power of the recovered polymer structure in reusability.

FT-IR analysis was performed to investigate the functional groups of the recycled catalyst. The results showed no changes in the spectrum of the recycled catalyst compared to the original one, confirming the high stability and preservation of the PC4RA@SiPr–OWO$_3$H structure under the applied reaction conditions (Fig. 9).
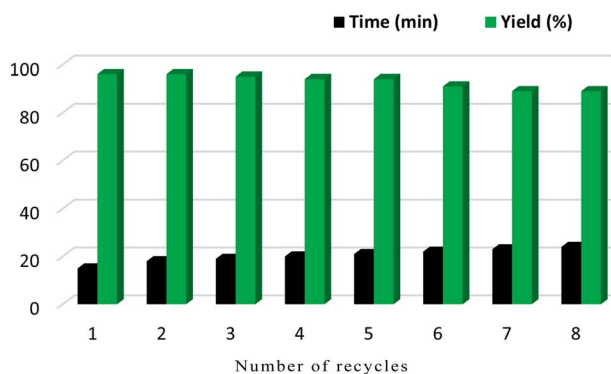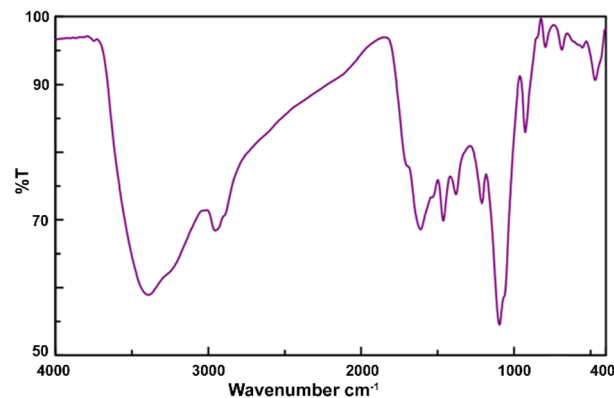

Fig. 9 FT-IR spectra of recovered PC4RA@SiPr–OWO$_3$H.

Further, by comparing the atomic ratios (C, O, Si, and W) of the recycled catalyst with the initial catalyst through EDX, it was found that PC4RA@SiPr–OWO$_3$H did not change significantly after several recycling stages. All connections were satisfactory (Fig. 10). The element distribution was investigated in the recovered catalyst using elemental mapping analysis. The obtained results for recycled PC4RA@SiPr–OWO$_3$H were compared with those for fresh one, which confirmed that the uniform distribution of elements was maintained after eight-time recycling (Fig. 11).

Element	Weight %	Atomic %	Net Int
C K	32.46	44.47	111.49
O K	47.33	48.68	221.12
W K	10.07	0.90	30.55
Si K	10.15	5.94	248.74
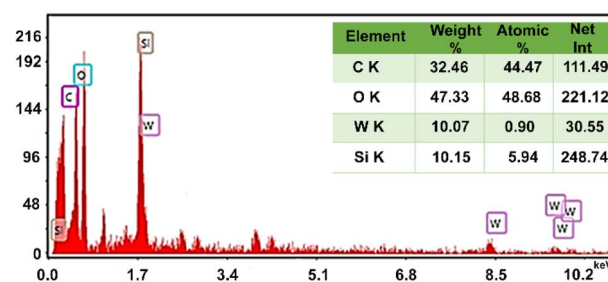
Fig. 10 EDX analysis of recovered PC4RA@SiPr–OWO$_3$H.

Fig. 8 Reusability of PC4RA@SiPr–OWO$_3$H as a catalyst in the synthesis reaction of 4H-pyran derivatives.
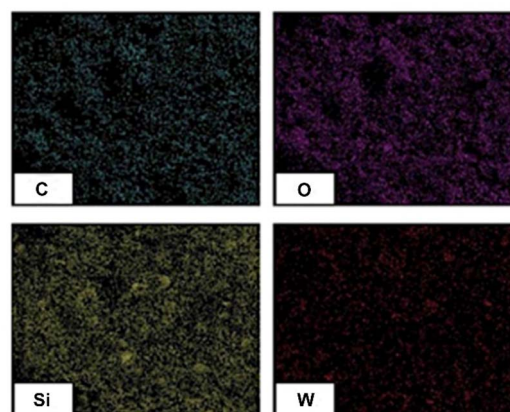

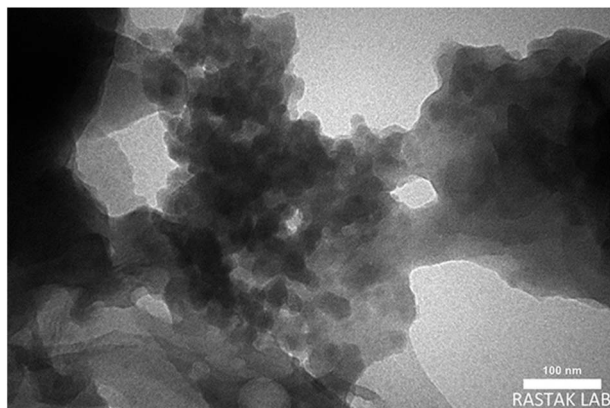Fig. 11 Elemental mapping of recovered PC4RA@SiPr–OWO$_3$H.

Fig. 12 TEM images of recovered PC4RA@SiPr–OWO$_3$H. Scale bar = 100 nm.

The permanence of the acidic part on the amorphous polymer surface after undergoing the eight cascade reactions and repeating stages of recycling was recorded through the TEM image and compared with the initial results, introducing a catalyst with high recyclability and resistance under applied conditions (Fig. 12).

Procedure for the acidity determination of PC4RA@SiPr–OWO$_3$H

First, 25 ml of a solution of NaCl (1 M) was taken and its pH was set at 6.3 as an elementary pH. Then, 0.05 g of the prepared catalyst was added to the above-mentioned aqueous solution under stirring at the environment temperature overnight. After spending this time, the recorded pH showed the number 2.7, demonstrating ion-exchanging between sodium ions and –OWO$_3$H protons, equivalent to the loading of –OWO$_3$H functionalities (H$^+$) on the desired catalyst surface computed around 0.9 mmol g^{-1}. Moreover, a back-titration analysis of this catalyst was relatively consistent with the above-mentioned result, which confirmed it.

An experimental procedure for the leaching test

Finally, a leaching test was carried out in the prepared 4H-pyran compounds to investigate whether PC4RA@SiPr–OWO$_3$H operates homogeneously or heterogeneously. To achieve this objective, after 50% reaction progress, the solid catalyst was isolated by filtration, and then the remaining were left to keep reacting under optimal conditions. Since it was not far from the expectation, no significant conversion was developed in the crude mixture after about 24 h, implying that the studied catalyst works in a heterogeneous state. These investigations excellently reveal the high durability of the polymeric catalyst in recoverability and reusability.

Conclusions

In this research, we have successfully synthesized heterogeneous PC4RA@SiPr–OWO$_3$H. FT-IR spectra confirmed the presence of the expected functional groups including tungstic acid as the catalytic centre. XRD analysis determined the amorphous structure of the polymer catalyst. The uniform distribution and atomic ratio of the constituents of the catalyst were checked and confirmed by mapping analysis and EDX, respectively. The thermal resistance of the functionalized polymer was tested by TG catalysis, which showed high stability up to a temperature of 650 °C. FE-SEM images confirmed the settlement of nanoparticles with a 55 nm average size on the polymer surface. Moreover, TEM proved the correct connection of the inorganic part to the amorphous polymer support. To show the catalyst efficiency, we used it in the synthesis of several 4H-pyran heterocycles. The stability of the catalyst after running eight continuous recycles was confirmed by FT-IR spectroscopy, EDX, mapping and TEM. The obtained results indicated the high capability of this catalyst to perform multi-component reactions in a one-pot manner and no need to activate intermediate products. High efficiency, simplicity of the separation path from the reaction environment, the ability to reuse the catalyst without reducing the catalytic power up to 8 times and more, and the property of guest-host are the main features reported in this study.

Conflicts of interest

There are no conflicts to declare.

Acknowledgements

References

1 C. Gropp, B. L. Quigley and F. Diederich, *J. Am. Chem. Soc.*, 2018, **140**, 2705–2717.

2 A. S. Thakar, H. M. Parekh, P. B. Pansuriya, H. B. Friedrich and G. E. Maguire, *Eur. J. Org. Chem.*, 2014, **2014**, 4600–4609.

3 B. S. Creaven, D. F. Donlon and J. McGinley, *Coord. Chem. Rev.*, 2009, **253**, 893–962.

4 M. Stödeman and N. Dhar, *Thermochim. Acta*, 1998, **320**, 33–38.

5 J. Vicens and V. Böhmer, *Calixarenes: a versatile class of macrocyclic compounds*, Springer Science & Business Media, 2012.

6 J. Vicens, J. Harrowfield and L. Baklouti, *Calixarenes in the Nanoworld*, Springer, 2007.

7 A. Dondoni, A. Marra, M. Rossi and M. Scoponi, *Polymer*, 2004, **45**, 6195–6206.

8 L. Y. Zakharova, Y. R. Kudryashova, N. M. Selivanova, M. A. Voronin, A. R. Ibragimova, S. E. Solovieva, A. T. Gubaidullin, A. I. Litvinov, I. R. Nizameev and M. K. Kadirov, *J. Membr. Sci.*, 2010, **364**, 90–101.

9 S. Memon, M. Tabakci, D. M. Roundhill and M. Yilmaz, *Polymer*, 2005, **46**, 1553–1560.

10 A. B. Mirgorodskaya, E. I. Yackevich, Y. R. Kudryashova, R. R. Kashapov, S. E. Solovieva, A. T. Gubaidullin,

I. S. Antipin, L. Y. Zakharova and A. I. Konovalov, *Colloids Surf., B*, 2014, **117**, 497–504.

11 A. I. Costa, H. D. Pinto, L. F. Ferreira and J. V. Prata, *Sens. Actuators, B*, 2012, **161**, 702–713.

12 H. Li, H. Huang, X. Yan, C. Liu and L. Li, *Mater. Chem. Phys.*, 2021, **263**, 124295.

13 A. A. Memon, A. R. Solangi, S. Memon, A. A. Bhatti and A. A. Bhatti, *Polycyclic Aromat. Compd.*, 2016, **36**, 106–119.

14 A. Gorbunov, N. Ozerov, M. Malakhova, A. Eshtukov, D. Cheshkov, S. Bezzubov, V. Kovalev and I. Vatsouro, *Org. Chem. Front.*, 2021, **8**, 3853–3866.

15 A. Ovsyannikov, S. Solovieva, I. Antipin and S. Ferlay, *Coord. Chem. Rev.*, 2017, **352**, 151–186.

16 Z. Lai, T. Zhao, J. L. Sessler and Q. He, *Coord. Chem. Rev.*, 2020, **425**, 213528.

17 L. Y. Zakharova, V. V. Syakaev, M. A. Voronin, F. V. Valeeva, A. R. Ibragimova, Y. R. Ablakova, E. K. Kazakova, S. K. Latypov and A. I. Konovalov, *J. Phys. Chem. C*, 2009, **113**, 6182–6190.

18 W. Gareth, *Chem. Commun.*, 2005, 892–894.

19 O. Pietraszkiewicz and M. Pietraszkiewicz, *J. Inclusion Phenom. Macrocyclic Chem.*, 1999, **35**, 261–270.

20 Y. Yamakawa, M. Ueda, R. Nagahata, K. Takeuchi and M. Asai, *J. Chem. Soc., Perkin Trans. 1*, 1998, 4135–4140.

21 M. H. Noamane, S. Ferlay, R. Abidi and M. W. Hosseini, *Tetrahedron*, 2017, **73**, 4259–4264.

22 M. Tabakci, S. Memon, M. Yilmaz and D. M. Roundhill, *React. Funct. Polym.*, 2004, **58**, 27–34.

23 J. A. Gajjar, R. H. Vekariya and H. M. Parekh, *Synth. Commun.*, 2020, **50**, 2545–2571.

24 W. F. de Paiva, I. B. Braga, J. V. de Assis, S. M. B. Castañeda, Á. G. Sathicq, V. Palermo, G. P. Romanelli, R. Natalino, M. J. da Silva and F. T. Martins, *Tetrahedron*, 2019, **75**, 3740–3750.

25 R. Warias, A. Zaghi, J. J. Heiland, S. K. Piendl, K. Gilmore, P. H. Seeberger, A. Massi and D. Belder, *ChemCatChem*, 2018, **10**, 5382–5385.

26 J. Zhang, M. Zhang, K. Tang, F. Verpoort and T. Sun, *Small*, 2014, **10**, 32–46.

27 A. Mouradzadegun, S. Elahi and F. Abadast, *RSC Adv.*, 2014, **4**, 31239–31248.

28 S. Wang, Y. Bi, X. Hang, X. Zhu and W. Liao, *Z. Anorg. Allg. Chem.*, 2017, **643**, 160–165.

29 J. De Assis, P. Abranches, I. Braga, O. Zuñiga, A. Sathicq, G. Romanelli, A. Sato and S. Fernandes, *RSC Adv.*, 2016, **6**, 24285–24289.

30 Z. Zhang, L. Li, D. An, H. Li and X. Zhang, *J. Mater. Sci.*, 2020, **55**, 1854–1864.

31 Z. Ding, J. Zhao, Z. Hao, M. Guo, L. Li, N. Li, X. Sun, P. Zhang and J. Cui, *J. Hazard. Mater.*, 2022, **423**, 127034.

32 L. Yang, X. Ran, L. Cai, Y. Li, H. Zhao and C.-P. Li, *Biosens. Bioelectron.*, 2016, **83**, 347–352.

33 R. Yuan, Z. Yan, A. Shaga and H. He, *Sens. Actuators, B*, 2021, **327**, 128949.

34 Z. Liu, X. Dai, Y. Sun and Y. Liu, *Aggregate*, 2020, **1**, 31–44.

35 Z.-L. Zhong, C.-P. Tang, C.-Y. Wu and Y.-Y. Chen, *J. Chem. Soc., Chem. Commun.*, 1995, 1737–1738.

36 S. Khaksar, A. Rouhollahpour and S. M. Talesh, *J. Fluorine Chem.*, 2012, **141**, 11–15.

37 B. Maleki and S. Sheikh, *Org. Prep. Proceed. Int.*, 2015, **47**, 368–378.

38 M. S. Esmaeili, M. R. Khodabakhshi, A. Maleki and Z. Varzi, *Polycyclic Aromat. Compd.*, 2021, **41**, 1953–1971.

39 E. A. A. Hafez, M. H. Elnagdi, A. G. A. Elagamey and F. M. A. A. El-Taweel, *Heterocycles*, 1987, **26**, 903–907.

40 P. Prasanna, S. Perumal and J. C. Menéndez, *Green Chem.*, 2013, **15**, 1292–1299.

41 M. Boominathan, M. Nagaraj, S. Muthusubramanian and R. V. Krishnakumar, *Tetrahedron*, 2011, **67**, 6057–6064.

42 B. Kazemi, S. Javanshir, A. Maleki, M. Safari and H. R. Khavasi, *Tetrahedron Lett.*, 2012, **53**, 6977–6981.

43 A. Molla and S. Hussain, *RSC Adv.*, 2014, **4**, 29750–29758.

44 A. Maleki and S. Azadegan, *J. Inorg. Organomet. Polym. Mater.*, 2017, **27**, 714–719.

45 K. Pradhan, S. Paul and A. R. Das, *Catal. Sci. Technol.*, 2014, **4**, 822–831.

46 S. J. Rezaei, A. M. Malekzadeh, A. Ramazani and H. Niknejad, *Curr. Drug Delivery*, 2019, **16**, 839–848.

47 H. H. Mardhiah, H. C. Ong, H. Masjuki, S. Lim and H. Lee, *Renewable Sustainable Energy Rev.*, 2017, **67**, 1225–1236.

48 L. M. Tunstad, J. A. Tucker, E. Dalcanale, J. Weiser, J. A. Bryant, J. C. Sherman, R. C. Helgeson, C. B. Knobler and D. J. Cram, *J. Org. Chem.*, 1989, **54**, 1305–1312.

49 H. Altshuler, E. Ostapova, O. Fedyaeva, L. Sapozhnikova and O. Altshuler, *Macromol. Symp.*, 2002, **181**, 1–4.